Scientific Research Publishing

Open Journal of Applied Sciences, 2025, 15(8), 2479-2502
https://www.scirp.org/journal/ojapps
ISSN Online: 2165-3925
ISSN Print: 2165-3917

Water-Regime Effects on Greenhouse Gas Emissions from Plant-Less, Silt-Loam Mesocosms in the Greenhouse

Cassandra Seuferling*, Diego Della Lunga, Jonathan Brye, Thomas Dockery, Kristofor Brye, Lisa Wood

Department of Crop, Soil, and Environmental Science, University of Arkansas, Fayetteville, Arkansas, USA
Email: *cs262@uark.edu, ddellalu@uark.edu, brye@uark.edu, tdockery@uark.edu, kbrye@uark.edu, lswood@uark.edu

How to cite this paper: Seuferling, C., Della Lunga, D., Brye, J., Dockery, T., Brye, K. and Wood, L. (2025) Water-Regime Effects on Greenhouse Gas Emissions from Plant-Less, Silt-Loam Mesocosms in the Greenhouse. *Open Journal of Applied Sciences*, **15**, 2479-2502.
https://doi.org/10.4236/ojapps.2025.158165

Received: July 11, 2025
Accepted: August 25, 2025
Published: August 28, 2025

Abstract

Evaluation and understanding of processes affecting atmospheric greenhouse gas (GHG) concentrations from the soil surface are critical to mitigating global climate change, particularly from the agricultural sector and the impact of soil-water regimes. The objectives of this study were to assess GHG [*i.e.*, carbon dioxide (CO_2), methane (CH_4), and nitrous oxide (N_2O)] emissions, evaluate soil oxidation-reduction (redox) potential (Eh), and track water-soluble (WS) nutrient changes under differing water regimes [*i.e.*, flooded (FL), intermittent wet and dry (IWD), seasonally flooded (SFL)] in silt-loam-textured mesocosms in the greenhouse. Soil Eh was measured hourly via redox sensor, GHG concentrations were collected weekly using vented, closed-chamber sampling with gas chromatography analysis, and soil samples were collected five times during the study period from January to April 2025. Greater fluctuations of GHGs and Eh were observed in IWD and SFL mesocosms. Carbon dioxide was the only gas with statistical differences among GHG emissions and was greatest ($P < 0.05$) from IWD (3.99 $Mg{\cdot}ha^{-1}$) and the lowest from FL (0.30 $Mg{\cdot}ha^{-1}$) mesocosms. Water soluble phosphorus was the greatest (4.1 $mg{\cdot}kg^{-1}$) from IWD, and the lowest from SFL (3.5 $mg{\cdot}kg^{-1}$) and FL (3.2 $mg{\cdot}kg^{-1}$). Water soluble magnesium and redox-active elements (*i.e.*, manganese, iron, sulfur) differed ($P < 0.05$) between water regime and time. Results determined water management practices can impact biogeochemical processes in multiple ways. The investigation of soil resource properties under various water regimes could better inform future management practices to improve nutrient and water efficiency, reduce greenhouse gas emissions, and enhance soil health.

Keywords

Water Regime, Greenhouse Gases, Climate Change, Water-Soluble Nutrients

1. Introduction

Atmospheric greenhouse gas (GHG) concentrations have increased since the pre-Industrial Era due to anthropogenic activities, leading to deleterious impacts of climate change [1]. Carbon dioxide (CO_2), methane (CH_4), and nitrous oxide (N_2O) are the GHGs of interest often analyzed as major climate-change contributors. In the context of soils, soil surface CO_2 emissions occur as a result of aerobic microbial and root respiration [2] [3]. Methane emissions from the soil surface occur from specialized soil microorganisms (*i.e.*, methanogens) in anaerobic, or water-logged, conditions [4], and generally only occur after all of the common electron acceptors in the soil and soil solution [*i.e.*, oxygen (O_2), nitrite (NO_2^-), manganese (Mn^{2+}), iron (Fe^{2+}), and sulfate (SO_4^{2-})] are depleted [5]. Nitrous oxide emissions are a result of denitrification, or the reduction of nitrate (NO_3^-) or NO_2^- to dinitrogen (N_2), nitrogen monoxide (NO), and/or N_2O by soil organisms in O_2-limited to anaerobic conditions [6] [7]. The development of mitigation practices, aimed to reduce GHGs released from soil, needs to be calibrated to several factors within the pedosphere-atmosphere continuum that control GHG production and release [8]. Climate change can also affect inputs and outputs of the water cycle (WC) [9]. Greater temperatures increase evaporation and transpiration rates of plants [9]. Warmer air, caused by the greenhouse effect, can hold more water vapor, which increases the volume and intensity of rainfall events leading to more flooded and saturated soils [10]. These changes to the WC can produce possible feedback loops that affect water regime, rate of microbial respiration, and GHG emissions [11].

Among the environmental parameters affecting biogeochemical processes related to GHG production in soil, volumetric water content (VWC) and soil oxidation-reduction (redox) potential (Eh) play a fundamental role, creating conditions that can enhance or suppress the production of specific GHGs [12]. Ecosystem hydrology, often described in terms of VWC fluctuations, varies among ecosystems and climate regions, and is influenced by precipitation, groundwater, biota, and topography [13]. However, the impact that soil VWC can have on GHGs can be evaluated and generalized across different ecosystems based on the degree of soil wetness experienced [8].

The difference in CO_2 emissions among various water regimes can be attributed to different decomposition rates at different VWCs, which are also affected by soil nitrogen (N) availability and biomass production [14]. Water fills soil pores, leading to soil O_2 depletion and creates anaerobic conditions [13]. Flooded or saturated conditions limit gas diffusion in the soil and within the flood water at the soil surface, slowing GHG release from the pedosphere, while dry-soil conditions can limit the transport of soluble substrates, therefore, both dry and flooded conditions can result in reduced microbial activity and soil respiration [15]. Additionally, O_2 absence in saturated soil substantially limits organic material oxidation, decreasing soil respiration rates [16]. Hydrologic regimes characterized by alternate-wet-and-dry (AWD) phases create fluctuating anaerobic/aerobic condi-

tions in the soil, promoting soil respiration and the decomposition of soil organic matter (SOM), consequently affecting the amount of CO_2 produced and released into the atmosphere [17]. While anaerobic conditions can favor carbon (C) sequestration in the topsoil, persistent saturated conditions, at microsites or within an entire soil profile, can facilitate methanogenic activity and CH_4 production [16]. Nitrogen-gas production in the pedosphere requires O_2 and enough soil moisture to activate the various enzymatic activities related to nitrification-denitrification, in addition to transporting soluble C and N substrates toward microbial communities [18]. Therefore, the alternation of wet and dry soil conditions is typically conducive of N_2O production [18]. Overall, soil moisture conditions around 60% water-filled pore space (WFPS) maximizes soil respiration, between 80% - 90% WFPS maximizes nitrification-denitrification, and above 95% WFPS maximizes methanogenesis [19].

Soil inundated with water can dissolve ionic compounds, affecting not only the biological components of the pedosphere but also the chemical status of the soil [13]. Prolonged saturation alters the soil Eh and often creates anaerobic or reducing conditions [20]. Soil reduction occurs when soils are depleted of O_2 and microbial respiration processes utilize alternate electron acceptors other than O_2 [*i.e.*, N, Mn, Fe, sulfur (S), and C] [20]. Soil Eh can estimate the alternative electron acceptor present in the soil solution [20]. Certain electron acceptors (*i.e.*, Mn and Fe) provide visual evidence of reduction (*i.e.*, redoximorphic features), where oxidized Mn will appear black and oxidized Fe will appear reddish, but when reduced, both Mn and Fe are colorless and will reveal the soil's mineral grain color [20]. Soils with differing degrees of wetness will undergo variable transitional periods of Eh and redoximorphic features. Saturated soils often require at least two weeks to develop stable anaerobic or reducing conditions [20]. However, it should be noted that soil Eh measurements are sensitive to soil texture, humidity, and measurement method and are spatially variable, even within short distances [21]. Predicted soil Eh for specific electron acceptors also varies among measurement conditions and is related to the specific microbial community present, creating difficulties in precisely evaluating the control of soil Eh on GHG emissions [22]. Microbial metabolism is typically aerobic when the soil Eh is >400 mV and becomes fully anaerobic around −200 mV or lower, with N, Mn, Fe, and C reduction occurring from 400 to 0, 400 to 0, 200 to 0, and 0 to −400 mV, respectively [23].

Climate change may result in alterations to soil hydrology, impacting GHG production and release, change soil Eh and subsequent chemical reactions, and overall impact soil biota, which can further promote climate change [13]. The study of soil hydrology, GHG, and soil redox status is critical to understanding the impacts of the aforementioned factors within the pedosphere. Understanding mechanisms affecting biogeochemical processes responsible for GHG production under different soil water regimes, and how the processes are going to be impacted by climate change, can provide essential guidance to develop tailored mitigation practices.

Therefore, the objectives of this study were 1) to assess GHG (*i.e.*, CO_2, CH_4,

and N_2O) emissions, 2) evaluate soil Eh variations, and 3) track water-soluble (WS) nutrient changes under differing water management regimes [*i.e.*, flooded (FL), intermittent wetting and drying (IWD), seasonally flooded (SFL)] in silt-loam-textured mesocosms in the greenhouse. It was hypothesized that FL mesocosms would have greater CH_4 fluxes and emissions than the other water regimes due to constant water saturation and potential anaerobic conditions present, leading to methanogenesis, and reduction of electron acceptors; SFL mesocosms would have greater N_2O fluxes and emissions than the other water regimes due to the combination of persistent saturated and short-term aerobic conditions that enhance nitrification-denitrification; and IWD mesocosms would have the greatest CO_2 and the least CH_4 and N_2O fluxes and emissions because of greater microbial respiration from a lack of continuous flooding leading to simulated anaerobic conditions. It was hypothesized that CH_4 fluxes would be strongly negatively correlated with soil Eh in FL mesocosms and that N_2O and CO_2 fluxes would be moderately positively correlated with soil Eh in IWD mesocosms. It was also hypothesized that soluble nutrient concentrations [*i.e.*, potassium (K), calcium (Ca), magnesium (Mg), sodium (Na)] would experience the greatest and lowest decrease over time in IWD and FL mesocosms, respectively due to remobilization processes during drying phases for IWD. It was also hypothesized that redox-active elements (*i.e.*, Mn, Fe, S) would experience a greater concentration increase in the FL mesocosm and a lower concentration increase in IWD, due to more negative Eh in the FL mesocosm that could force reduction of elements. It was finally hypothesized that zinc (Zn) and phosphorus (P) concentrations would experience the greatest decrease in FL mesocosms, and the lowest decrease in IWD, due to adsorption and precipitation processes commonly occurring in flooded conditions [20].

2. Materials and Methods

2.1. Soil Collection and Mesocosm Preparation

The study was conducted between January and April 2025 in a greenhouse at the Agricultural Research and Extension Center (AREC), Fayetteville, AR. Soil was collected the previous fall from the top 10 cm of a silt-loam soil (fine-silty, mixed, active, thermic Typic Glossaqualfs) cropped to a rice (*Oryza sativa*)-soybean (*Glycine max*) rotation at the Pine Tree Research Station near Colt in east-central AR and from a private producer's silt-loam soil (fine-silty, mixed, active, thermic Aeric Epiaqualfs) cropped to soybean near Tillar in southeast AR. Moist soil was sieved through a 6-mm mesh screen to simulate mixing by tillage. As there was not sufficient mass of soil from either individual soil, the two silt-loam soils were thoroughly mixed together and air-dried for several weeks on a greenhouse bench at ~30˚C. The two soils shared similar characteristics; therefore, the mixing process did not substantially alter physical soil properties.

Twelve, 0.023-m^3 plastic tubs (*i.e.*, mesocosms) were assembled on a single bench on 30 January, 2025 [day of year (DOY) 30] by thoroughly hand-mixing 20

kg of the air-dried soil mixture with 3.5 kg of commercially obtained composted peat and animal manure (Garden Magic Compost and Manure, Michigan Peat Co, Houston, TX). The organic compost was added to provide enough organic, labile, C-containing material to stimulate microbial response to the established soil moisture treatments. The low level of soil fertility commonly observed in intensively cultivated fields could have limited microbial processes if organic addition was not implemented [1]. The weight and measured volume of the soil-compost mixture were used to calculate the soil bulk density (BD) in each mesocosm. Water-regime treatments (*i.e.*, IWD, SFL, and FL) were assigned to each mesocosm in a completely random design (CRD) with four replicates per water regime. To monitor soil Eh over time, on 6 February, 2025 (DOY 37), a redox sensor (Model S65OKD-ORP, Sensorex, Garden Grove, CA) was installed in each mesocosm in a vertical orientation at a 4-cm depth from the soil surface, while water content reflectometers (Model CS616, Campbell Scientific, Inc., Logan, UT) were installed in a horizontal orientation at the 10-cm depth in all mesocosms, except in the FL treatment replicates, to monitor soil VWC over time. Since FL mesocosms were constantly flooded (described below), a reflectometer was not necessary. All the sensors were connected to a datalogger (CR 1000, Campbell Scientific) powered by an external 12-V battery and set to scan the sensors every 5 minutes and record data as an hourly average. Therefore, each sensor recorded 24 data points per day. On 10 February, 2025 (DOY 41), sensors and dataloggers began recording data.

After sensor installation, a 30-cm diameter by 30-cm tall polyvinyl chloride (PVC) base collar was installed in each mesocosm to facilitate weekly GHG measurements (described below). Base collars were installed to the bottom of the mesocosms, roughly a depth of 12 cm, in a position that did not interfere with the installed sensors. To allow for water flow in and out of the base collars, each base collar had four, 12.5-mm-diameter holes at 12 cm up from the beveled bottom. After base collar installation, the holes were located right at the soil surface.

2.2. Water Regimes

After soil-compost mixture addition, mesocosms were kept visibly moist from 6 to 9 February 2025 (DOY 37 to 40) to allow the soil to settle. On 10 February 2025 (DOY 41), the water-regime treatments were established. The mesocosms under FL and SFL were flooded on 10, February 2025 (DOY 41). The flood in the FL mesocosms was maintained at a depth of at least 4 cm until termination of the study on 3 April 2025 (DOY 93). The flood in the SFL-mesocosms was maintained at a dept of 4 cm from 10 to 24 February, 2025 (DOY 41 to 55), at which time the SFL mesocosms were left to dry until 12 March 2025 (DOY 71) for what was considered the first drying cycle. The flood was re-established in the SFL mesocosms on 13 March 2025 (DOY 72) and maintained until 26 March 2025 (DOY 85), at which time the second drying cycle started and lasted until the end of the study (*i.e.*, 3 April 2025; DOY 93). The IWD mesocosms were watered to maintain a

constant VWC of 0.56 $cm^3 \cdot cm^{-3}$ slightly below saturation (*i.e.*, 0.58 $cm^3 \cdot cm^{-3}$). Mesocosms under the IWD water regime followed the same wet and dry cycles as for the SFL mesocosms. All mesocosms were watered on a regular schedule, three times per week, except during the drying cycles. In order to water the IWD mesocosms, the VWC was measured with a Theta Probe (HH150 Moisture Meter and SM150T Moisture Sensor, Delta-T Devices, Cambridge, England), then, using the estimated bulk density, VWC converted to gravimetric water content and then again to milliliters of water necessary to reach the desired target VWC in each of the IWD mesocosms. Since no plants were in the mesocosms, evaporation was the only process of water removal from the mesocosms. A primary and secondary heating/cooling system kept the diurnal and nocturnal temperature in the greenhouse at 31˚C and above 22˚C, respectively, for the duration of the study.

2.3. Soil Sampling and Analyses

Initial soil properties were characterized after mixing the two silt-loam soils together, but before the organic compost was added. Three soil sub-samples were collected from the mixture during the air-drying process. Soil sub-samples were oven-dried at 70˚C for at least 48 hours, mechanically ground, and sieved through a 2-mm mesh screen. Mehlich-3 extractable soil nutrient concentrations (*i.e.*, P, K, Ca, Mg, Fe, Mn, Na, S, and Zn) were determined in a 1:10 soil mass:extractant volume ratio and analyzed by inductively coupled, argon-plasma spectrophotometry (ICAPS; Spectro Arcos ICP, Spectro Analytical Instruments, Inc., Kleve Germany) [24]. Weight-loss-on-ignition after combustion at 360˚C for 2 hours [24] was used to determine SOM concentration.

Additional soil samples were collected from each mesocosm every two weeks during the study period [*i.e.*, 12 and 25 February, 11 and 25 March, and 2 April, 2025 (DOY 43, 56, 70, 84, and 92)] to characterize WS nutrient fluctuations. Two soil cores were collected in mesocosms on each of the five soil sampling dates using 5-mm diameter copper tubes. Soil cores were representative of the entire mesocosm soil depth and were collected outside the GHG sampling base collar to avoid soil disturbance impacting GHG analysis. Samples were oven-dried at 70˚C for at least 48 hours and manually ground in a mortar and pestle and sieved through a 2-mm mesh screen. Similar to procedures for Mehlich-3-extractable soil nutrients, WS nutrient (*i.e.*, P, K, Ca, Mg, Na, S, Fe, Mn, and Zn) concentrations were determined in a 1:10 soil mass:water volume ratio and analyzed by ICAPS.

2.4. Greenhouse Gas Measurements

Gas sampling procedure followed the methodology outlined by [25]. Gas sampling occurred weekly from 13 February to 3 April 2025, (DOY 44 to 93) for a total of eight gas sampling dates. Before sampling, rubber stoppers 1.3 cm in diameter (part #73828A-RB, Voigt Global, Lawrence, KS) were placed in the four holes at the soil surface in the base collars. A 30-cm-diameter, 10-cm-tall PVC cap, with a 2.5-cm^2 fan (MagLev GM1202PFV2-8, Sunon Inc., Brea, CA) installed

on the underside for headspace gas mixing and 15-cm-long, 0.63-cm-inside-diameter copper refrigerator tube to maintain pressure equilibrium between inside and outside the chamber, was placed on the base collars, sealed with a rubber flap to create an air-tight, closed-headspace chamber. Gas samples were collected from each chamber using a syringe and transferred into a pre-capped, pre-evacuated, 10-mL glass vial (part #5183-4479 and part #5182-0838, Agilent Technologies, Santa Clara, CA) once every 30 minutes over a period of one hour (*i.e.*, 0, 30, and 60 min). A portable meteorological station (S/N: 182090284, Control Company, Webster, TX) was used to record the ambient air temperature and barometric pressure at the start of each sampling event. Gas samples were analyzed using a Shimadzu GC-2014 ATFSPL 115 V gas chromatograph (GC; Shimadzu North America/Shimadzu Scientific Instruments Inc., Columbia, MD), with a flame ionization detector coupled with a methanizer for CH_4 and CO_2, and an electron capture detector for N_2O concentrations.

Gas fluxes were determined from the change in gas concentration over the 60-min measurement interval by determining the best-fit linear regression slope across the 0-, 30-, and 60-min concentrations for each mesocosm on each sample date (Microsoft Excel v. 2503, Microsoft, Redmond, WA). The regression slope was then multiplied by the measured chamber volume and divided by chamber surface area to obtain gas flux ($\mu L \cdot m^{-2} \cdot min^{-1}$) for each gas (*i.e.*, CO_2, CH_4, and N_2O). Following previous studies [26]-[28], fluxes < 0 were reassigned the value of 10^{-6}, which represented the detection limit of the GC-2014. Season-long GHG emissions ($Mg \cdot ha^{-1}$ for CO_2, $kg \cdot ha^{-1}$ for CH_4 and N_2O) were calculated by linear interpolation between fluxes on consecutive sampling dates for each mesocosm. Global warming potential (GWP) was calculated for each mesocosm using the conversion factors of 28 and 265 for CH_4 and N_2O, respectively [1].

2.5. Statistical Analyses

Based on a CRD repeated-measures, a two-factor analysis of variance (ANOVA) was used to evaluate the effects of water regime (*i.e.*, FL, IWD, and SFL), time (*i.e.*, weekly sampling dates), and their interactions on GHG (*i.e.*, CO_2, CH_4, and N_2O) fluxes and WS soil nutrient (*i.e.*, P, K, Ca, Mg, Na, S, Fe, Mn, and Zn) concentrations using the ASREML package (version 4.1.0.90) in R (version 4.3.2, R Foundation for Statistical Computing, Vienna, Austria). Water regime and time were considered fixed effects. Restricted maximum likelihood (REML) was used as the convergence method for the model, where different distributions (*i.e.*, normal and gamma) and variance-covariance structures (*i.e.*, identity, compound symmetry, diagonal, autoregressive first and second order, and unstructured) for the residuals were evaluated. Each model was assessed with heteroskedasticity and homoskedasticity. The Akaike information criteria (AIC) and the likelihood ratio test (LRT) were used to determine the best fit. As a result, all response variables were characterized by a normal distribution and homogeneity of variance, with a variance-covariance structure of the residuals modeled as identity for the three

GHGs and all WS nutrients, except for Fe and Mn concentrations whose residuals were modeled with an autoregressive first order matrix. Each response variable dataset was complete and balanced and the visual analysis of externally studentized residuals showed no clear outliers.

Wald tests were performed on the best-fit models to extract the ANOVA results for the fixed effects. Pairwise, multiple comparisons were made using Tukey's method. Soil Eh data were extracted from the 1-hr time period during which each actual GHG sampling occurred for each mesocosms. A simple linear correlation analysis was performed using JMP (version 14.3.0, SAS Institute, Inc., Cary, NC) to evaluate the relationships between GHG fluxes, separately by gas, and soil Eh for each water regime. A one-factor ANOVA was conducted in R to evaluate the effect of water regime on GHG emissions and GWP. Assumptions for the one-factor ANOVA were checked using the Shapiro's test for normality and Levene's test for homogeneity of variance. As a result, GHG emissions and GWP were normally distributed and characterized by homogeneity of variance. Significance for all tests was judged at $P < 0.05$.

3. Results and Discussion

3.1. Initial Soil Properties

Soil properties were assessed at the beginning of the study and used to characterize the soil from an agronomic perspective. Based on general agronomic soil recommendations from the University of Arkansas Division of Agriculture, soil nutrient concentrations of K (111 $mg \cdot kg^{-1}$) and Zn (2.0 $mg \cdot kg^{-1}$) were sub-optimal, P (35.3 $mg \cdot kg^{-1}$) was optimal, and Ca, Mg, S, and Mn (1214, 280.7, 14.3, and 145.3 $mg \cdot kg^{-1}$ respectively) were above levels recommended for agricultural practices (**Table 1**) [29]. Soil nutrients concentrations determined that the soil represented a typical Arkansas soil under prolonged cultivation [29]. Iron concentrations were considered elevated and close to toxic levels for crops (*i.e.*, >300 $mg \cdot kg^{-1}$; **Table 1**) [29]. The presence of moderately high concentrations of Fe, Mn, and S created an ideal environment for soil redoximorphic activity [20]. Soil organic matter was low for row-crop agriculture production (1.6%), where recommendations indicate an ideal level for agricultural activity to be at or above 2.0% (**Table 1**) [29]. The addition of organic compost provided additional C substrate for microbial processes to occur at a relatively short timescale (*i.e.*, eight weeks).

3.2. Soil VWC

Reflectometer-recorded VWC for IWD and SFL mesocosms were averaged across mesocosm replication, and FL mesocosms were reported as 0.56 $cm^3 \cdot cm^{-3}$ to represent saturated VWC (**Figure 1**). Both IWD and SFL mesocosms followed similar trends, with the magnitude of SFL being consistently greater than IWD. At the beginning of the study, during the first wet cycle (10 to 24 February; DOY 41 to 55), both IWD and SFL mesocosms' VWC gradually decreased initially,

Table 1. Summary of initial soil chemical properties (n = 3) from the silt-loam-soil mixture used for the 2025 greenhouse study.

Soil Property	Mean (± standard error)
Mehlich-3 extractable nutrients ($mg \cdot kg^{-1}$)	
P	35.3 (0.7)
K	111 (6)
Ca	1214 (11.6)
Mg	280.7 (2.7)
S	14.3 (0.3)
Fe	210 (1.7)
Na	33.3 (0.3)
Mn	145.3 (0.9)
Zn	2.0 (<0.1)
Soil organic matter (%)	1.6 (<0.1)

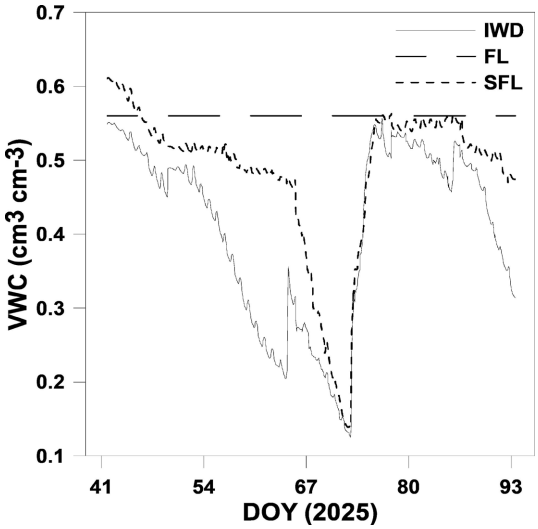

Figure 1. Soil volumetric water content (VWC) measured at the 10-cm soil depth over time by day of year (DOY) by water regime [*i.e.*, intermittent wetting and drying (IWD), flooded (FL), and seasonally flooded (SFL)] for the 2025 greenhouse study.

followed by a more uniform and stabilized trend, possibly due to the assessment of percolating water within the tubs during the first water applications (Figure 1). As anticipated, VWC from the IWD and SFL mesocosms decreased throughout the first drying cycle (25 February to 12 March; DOY 56 to 71) then rapidly increased at the start of the subsequent wet cycle (13 to 26 March; DOY 72 to 85), and gradually decreased at the final dry cycle until study termination (27 March to 3 April; DOY 86 to 93; Figure 1). The drying processes in the IWD mesocosms were visually more rapid than in the SFL mesocosms, highlighting the substantial difference in environmental conditions between saturated and flooded settings (Figure 1). Volumetric water contents for IWD and SFL mesocosms were visually

close in pattern to the inverse of IWD and SFL mesocosm Eh, likely due to the relationship between VWC and microbial respiration, indirectly linking VWC to soil Eh (Figure 1; Figure 2) [13] [23].

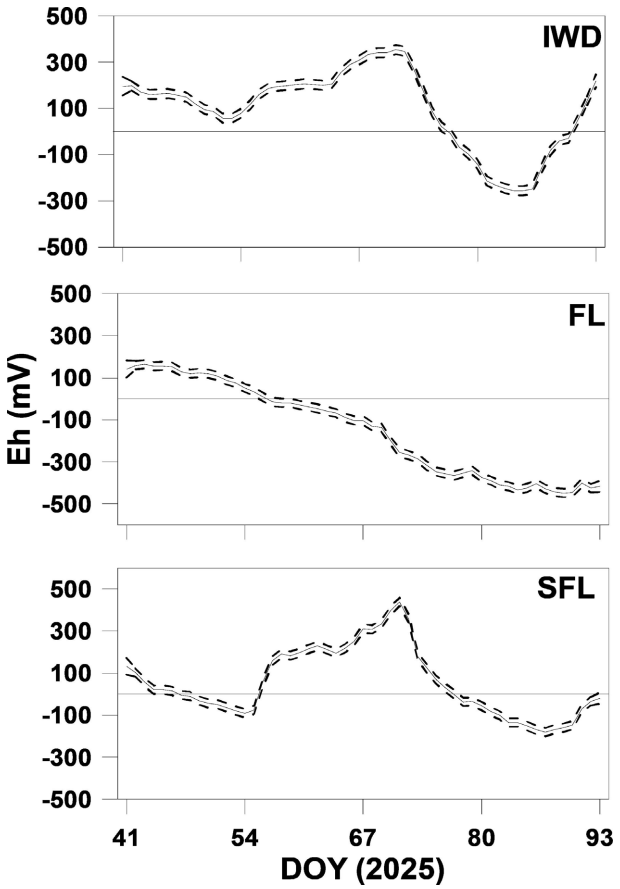

Figure 2. Soil oxidation-reduction potential (Eh) measured at the 4-cm soil depth over time by day of year (DOY) by water regime [*i.e.*, intermittent wetting and drying (IWD), flooded (FL), and seasonally flooded (SFL)] for the 2025 greenhouse study. Dashed lines around the solid line in each panel represent the 95% upper and lower confidence interval of the mean.

3.3. Soil Eh

Evaluation of soil Eh in each mesocosm resulted in visual and numeric similarities among IWD and SFL mesocosms that were characterized by wider fluctuations compared to the more constant Eh from FL mesocosm (Figure 2). Between the IWD and SFL mesocosms, as was observed for the VWC patterns, the magnitude of IWD fluctuations in soil Eh was numerically greater than that of SFL (Figure 2). Soil Eh from IWD and SFL mesocosms initially experienced a decreasing trend following the first wetting phase (10 to 24 February; DOY 41 to 55), then increased during the first drying phase (25 February to 12 March; DOY 56 to 71) followed by another Eh decrease during the subsequent wetting phase (13 to 26 March; DOY 72 to 85), and finally increased throughout the final drying phase (27 March to 3 April; DOY 86 to 93; Figure 2). The IWD mesocosms experienced aerobic

conditions (*i.e.*, Eh > 0 mV) for the majority of the study, except from DOY 72 to 85, when a negative soil Eh, was observed (**Figure 2**) [20] [23]. The lack of ponded water atop the soil surface in the IWD mesocosms, most likely allowed the infiltration of O_2 delaying and limiting the creation of a reducing environment (**Figure 2**) [30]. Soil redox potential in FL mesocosms followed a linear decrease from the start to the end of the study period, indicating that soil conditions were becoming more reduced as the study progressed, due to the lack of O_2 inputs and the consumption of alternative electron acceptors [31]. The soil Eh in the SFL mesocosm experienced reducing conditions in the last part of the first wet cycle and for the majority of the second wet cycle, most likely due to the higher VWC (**Figure 1**; **Figure 2**) [32].

3.4. Greenhouse Gas Fluxes

Across the three treatments (*i.e.*, IWD, SFL, and FL), based on visual observation, the temporal variation of the GHG fluxes showed distinct patterns across water regimes (**Figure 3**). Carbon dioxide fluxes remained substantially low in the FL mesocosms for the entire duration of the study most likely due to the constant presence of the ponding water that significantly limited aerobic respiration and the diffusion rate of gas molecules (**Figure 3**) [33]. Wider fluctuation of CO_2 was observed in IWD mesocosms, where a combination of aerobic and saturated conditions enhanced soil respiration processes (**Figure 1**; **Figure 3**) [28]. A single, discernible peak was observed from the SFL mesocosms on 13 March (DOY 72) when the flood was re-established, potentially caused by gas produced and accumulated in the soil profile during the dry cycle being pushed out (**Figure 1**; **Figure 3**) [34].

Somewhat similar to CO_2, the FL mesocosms reported relatively low and constant N_2O fluxes, while more variability was observed in the IWD mesocosms, where saturated and aerobic conditions most likely enhanced the coupled action of nitrification-denitrification (**Figure 1**; **Figure 3**) [35]. Similar to CO_2, the reintroduction of the flood on 13 March (DOY 72) in SFL mesocosms likely caused the only discernable peak of N_2O fluxes (**Figure 3**).

Likely related to the variability in environmental conditions throughout the greenhouse study, CO_2 and N_2O fluxes differed ($P < 0.05$) by treatment over time, while CH_4 fluxes differed ($P < 0.05$) only by treatment (**Table 2**). However, a significant difference among treatments was reported only at three sampling dates (27 February, 6 and 13 March; DOY 58, 65, and 72) for CO_2, and one sampling date (13 March; DOY 72) for N_2O (**Figure 3**). Contrary to that hypothesized, the peak CO_2 flux (1179 $g \cdot m^{-2} \cdot h^{-1}$) was measured on 13 March (DOY 72) from SFL mesocosms and was greater than CO_2 fluxes from both IWD and FL mesocosms on the same day (**Figure 3**). Similarly, and as hypothesized, peak N_2O flux (0.21 $mg \cdot m^{-2} \cdot h^{-1}$) was measured in the SFL mesocosms on 13 March (DOY 72), but was only greater than the flux reported from the FL mesocosms on the same day (**Figure 3**). Carbon dioxide fluxes were not significantly different ($P > 0.05$) than

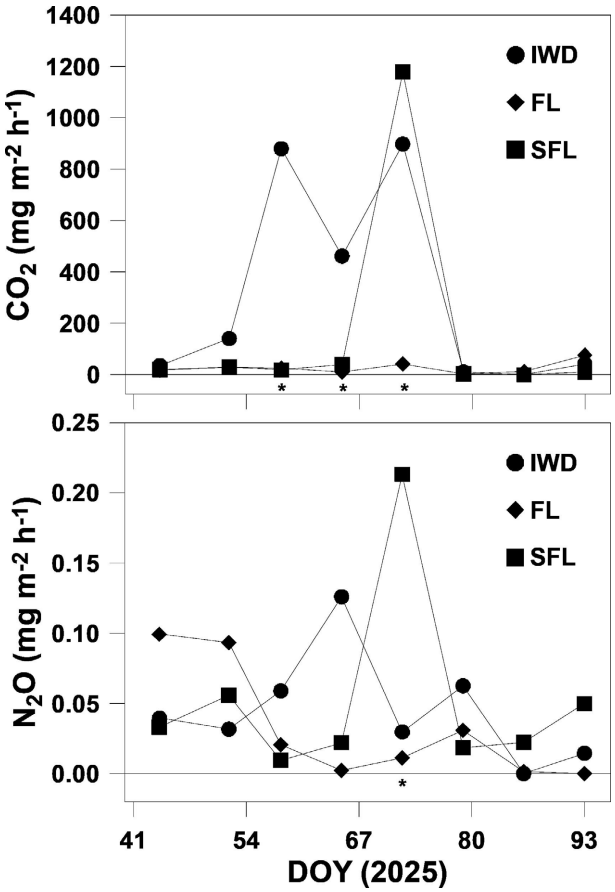

Figure 3. Carbon dioxide (CO_2) and nitrous oxide (N_2O) fluxes, reported as least square means, among water regimes [*i.e.*, intermittent wetting and drying (IWD), flooded (FL), and seasonally flooded (SFL)] over time by day of year (DOY) during the 2025 greenhouse study. Lines connecting data points are for graphical representation only. Asterisks (*) below the zero-flux line denote measurement dates when a significant ($P < 0.05$) difference occurred among treatments.

zero on all sampling dates except 3 April (DOY 93) and 13 March (DOY 72) for the FL and SFL mesocosms respectively. Intermittent wetting and drying treatment fluxes averaged among replicates, measured on February 13, 20 and 27 March, and 3 April (DOY 44, 79, 86 and 93 respectively) were not different ($P > 0.05$) than zero. Nitrous oxide fluxes measured on February 27, and March 6 and 20 (DOY 58, 65, and 79 respectively) in the IWD treatment, February 13 and 21 (DOY 44 and 52) in the FL treatment, and on March 13 (DOY 73) in the SFL treatment, were not different ($P > 0.05$) than zero.

As hypothesized, CH_4 fluxes averaged over weekly measurement dates were greatest in the FL mesocosms but did not differ ($P > 0.05$) from the SFL mesocosms (Figure 4). Methane fluxes were lowest in the IWD mesocosms but did not differ ($P > 0.05$) from the SFL mesocosms (Figure 4). The statistical similarities among water regimes could possibly be due to large variability of CH_4 fluxes among replicates in the SFL regime that created a large standard error in the statistical analysis. Soil heterogeneity and soil-gas-water pockets can form

Table 2. Analysis of variance summary of the effects of water-regime treatment, time (*i.e.*, measurement date), and their interaction on greenhouse gas [*i.e.*, carbon dioxide (CO_2), methane (CH_4), and nitrous oxide (N_2O)] fluxes for the 2025 greenhouse study.

Source of Variation	CO_2	CH_4	N_2O
		P	
Treatment	<0.01	0.02	0.49
Time	<0.01	0.51	0.18
Treatment × time	<0.01	0.24	<0.01

micro-conditions that allow for CH_4 formation in overall conditions that would not normally enhance methanogenesis [36]. Methane is also known to conglomerate as bubbles in situ within wetland soils [37]. It is possible that CH_4 formed under reducing conditions, was then fluxed out when oxidizing conditions returned, causing sporadic large values (*i.e.*, hot spots) that inflated the confidence interval of the averaged fluxes among sampling dates [37]. The lack of significant differences of CH_4 over time highlights how the three water regimes were characterized by different, but constant environmental conditions even when drying phases are added to the management practices, and suggest that water regimes divergent from flooded conditions can constitute a valid alternative to reduce methanogenesis in environments prone to substantial production of CH_4 like rice fields and wetlands (**Figure 4**) [38].

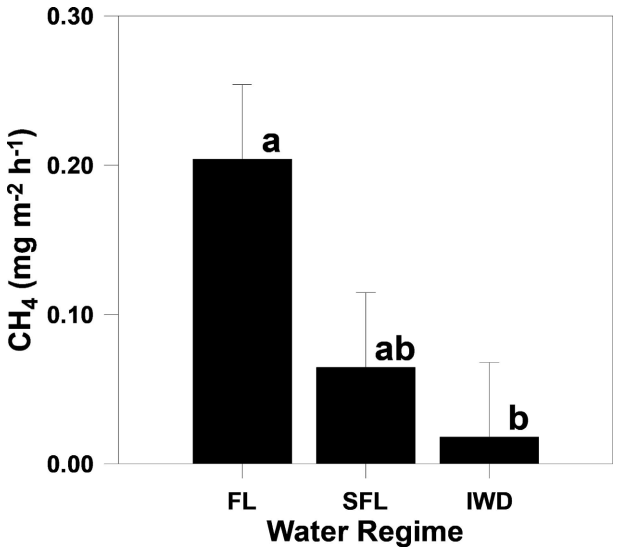

Figure 4. Methane (CH_4) fluxes, averaged over weekly measurement dates, among water regimes [*i.e.*, intermittent wetting and drying (IWD), flooded (FL), and seasonally flooded (SFL)] for the 2025 greenhouse study. Different lower-case letters atop bars denote a significant ($P < 0.05$) difference. Line on top of bars represents the standard error of Tukey's statistical analysis.

3.5. GHG Emissions and Global Warming Potential

Evaluation of GHG emissions across mesocosm water management regimes (*i.e.*,

IWD, SFL, FL) resulted in significant differences for CO_2 emissions ($P < 0.05$), but not for N_2O and CH_4 emissions ($P > 0.05$; Table 3). In accordance with that hypothesized, CO_2 emissions were greater in the IWD mesocosms (3.99 Mg·ha^{-1}) and significantly decreased in the SFL (2.17 Mg·ha^{-1}) and again in the FL (0.30 Mg·ha^{-1}) mesocosms (Table 3). Based on VWC and soil Eh trend across mesocosms, more aerobic conditions were experienced in the IWD compared to the SFL and FL, and SFL was more aerobic than FL, leading to greater rates of aerobic microbial respiration, therefore releasing CO_2 [2] [3]. A decreasing trend in soil-surface CO_2 release as soil moisture increased, often as a result of seasonal flooding or wetting events, has been reported in previous studies in wetland soils [39] [40].

In contrast to that hypothesized, CH_4 emissions did not statistically differ between IWD, SFL, and FL mesocosms ($P = 0.26$; Table 3). However, numerically, FL mesocosms' CH_4 emissions were 3 times greater than SFL, and 8.8 times greater than IWD mesocosms (Table 3), indicating greater, yet nonsignificant, CH_4 release from mesocosms with greater VWC. Studies evaluating varying wetland moisture conditions often conclude that, as VWC increases, soil-surface CH_4 release also increases [39] [40]. The lack of a significant difference in CH_4 emissions based on water management regime may be due to insufficient flooding duration or shallow soil depth to provide adequate prolonged reducing conditions for methanogenesis. The presence of a shallow flood most likely allowed some degree of O_2 infiltration, slowing the rate of reduction of the soil in the SFL and FL mesocosms [35].

Table 3. Analysis of variance summary of the effect of water regime [*i.e.*, intermittent wetting and drying (IWD), seasonally flooded (SFL) and flooded (FL)] on season-long gas [*i.e.*, carbon dioxide (CO_2), methane (CH_4), and nitrous oxide (N_2O)] emissions and global warming potential (GWP) for the 2025 greenhouse study. Mean (±standard error) are reported.

Water Regime	CO_2 (Mg·ha^{-1})	CH_4 (kg·ha^{-1})	N_2O (kg·ha^{-1})	GWP (Mg·ha^{-1})
IWD	3.99 (0.09) a[†]	0.27 (0.09)	0.61 (0.20)	4.17 (0.10) a
SFL	2.17 (0.09) b	0.79 (0.36)	0.63 (0.11)	2.35 (0.11) b
FL	0.30 (0.04) c	2.40 (1.5)	0.36 (0.10)	0.46 (0.03) c
P-value	<0.001	0.26	0.37	<0.001

[†]Means within a column with different lower-case letters are different at $P < 0.05$.

Similar to CH_4 emissions, N_2O emissions did not differ between IWD, SFL, and FL mesocosms ($P = 0.37$; Table 3). However, a numerical trend was observed, with SFL mesocosms characterized by the numerically greatest N_2O emissions, while FL had the numerically least N_2O emissions (Table 3), somewhat as hypothesized. Former research has shown N_2O emissions may increase with increases in soil WFPS [41] and water depth [42]. However, a multi-site study evaluating N_2O emissions and VWC determined VWC is not a sole predictor of N_2O emissions

due to the complexity of the N-cycle within soils, where N_2O production is the result of synergistic parameters including available N, soil temperature, soil texture, microbial communities, and VWC history [38]. The fluctuation of wetting and drying from SFL mesocosms may have allowed for nitrification and denitrification to produce N_2O, however, other aforementioned factors may have hindered a direct significant response to determine the predictive ability of water management regime on N_2O emissions (**Table 3**). Cultivated agricultural soils commonly lack N substrate that is compensated with fertilizer addition [1]. The lack of N input additions to mesocosms may have limited nitrification-denitrification processes, and therefore N_2O production.

Due to the magnitude of CO_2 emissions, calculated GWP values reported results similar to CO_2 emissions (**Table 3**). Similar to CO_2, GWP differed between IWD, SFL, and FL mesocosms ($P < 0.05$), with the greatest GWP in IWD mesocosms, and the least GWP in FL mesocosms (4.17 and 0.46 $Mg{\cdot}ha^{-1}$ respectively; **Table 3**). Per the results of GWP, increasing VWC can lead to lower GWP, potentially reducing the impact on global climate change. However, individual GHG evaluation is still necessary to determine the impact of gases with lower magnitudes than CO_2. Drier soil conditions can lose more C from the soil from CO_2 emissions than wet soils, indicating how appropriate water management is fundamental to reduce the loss of soil organic material which is considered one of the major indicators of soil health and soil fertility [43] [44].

3.6. Linear Regression Analyses

Linear regression analyses were conducted to determine the role of soil Eh in production and release of GHGs across water regimes (**Table 4**). The linear models explaining the variability of soil respiration were significant for the IWD and SFL mesocosms but not for the FL treatment (**Table 4**). However, soil Eh was a significant parameter only for the soil respiration model in the IWD mesocosms. As hypothesized, soil Eh was able to explain 29% of the variation of soil respiration in the IWD mesocosms that equated to a correlation coefficient (r) of 0.53 (**Table 4**). The RMSE was numerically lower than the standard deviation (SD) of the raw fluxes (376 $mg{\cdot}m^{-2}{\cdot}h^{-1}$), suggesting that the model predictions more closely captured the trend of the data compared to the general spread of the fluxes (**Table 4**). The linear regressing model for IWD suggests that each unit increase of soil Eh corresponds to a unit increase of CO_2 fluxes (**Table 4**). Regression models can be assessed only in relation to the range values of the predictors [45]. Considering that a general inverse relationship between soil VWC and soil Eh has been extensively evaluated [22], the model for CO_2 indicated that increases soil Eh, observed during the dry cycles in the current study, are associated with greater rate of soil respiration (**Figure 1**; **Figure 2**; **Table 4**).

Different from CO_2 and contrary to that hypothesized, the linear regression model for CH_4 in the FL mesocosms was the only model that was overall significant and with a significant parameter (**Table 4**). The CH_4 linear regression model

was able to explain 14% of the variability of the data with a moderate positive r coefficient equal to −0.38 and a RMSE numerically lower than the SD of the flux data in the FL mesocosms (0.46 mg·CH_4·m^{-2}·h^{-1}, Table 4). The model indicated that a unit increase of soil Eh corresponds to a 0.01 decrease in CH_4 production (Table 4). Similar results were reported in rice production systems under various water management practices [28] [46] [47].

Similar to CO_2, and contrary to what hypothesized, among the linear models for N_2O, only the SFL and FL mesocosms reported an overall significant regression model and a significant predictor parameter (Table 4). The SFL and FL models were able to explain 15% (r = 0.39) and 24% (r = 0.49) of the variability of the data within mesocosms, respectively (Table 4). The IWD regression model had numerically lower RMSE compared to SD for the SFL (0.08 mg·N_2O·m^{-2}·h^{-1}) and the FL (0.06 mg·N_2O·m^{-2}·h^{-1}) mesocosms (Table 4). Both SFL and FL regression models indicated that a unit increase of soil Eh corresponds to a 0.01 increase in N_2O production (Table 4). A positive relationship between soil Eh and N_2O has been reported in previous studies [46] [48], where production of N_2O was recorded in a wide range of soil Eh between 400 mV and −200 mV [48], although the greatest rate of nitrification-denitrification was determined between 100 mV and −100 mV [46].

Table 4. Summary of linear regression analyses to predict carbon dioxide (CO_2), methane (CH_4), and nitrous oxide (N_2O) fluxes (n = 96) separately by water regime [*i.e.*, intermittent wetting and drying (IWD), seasonally flooded (SFL), and flooded (FL)] from soil oxidation-reduction potential (Eh) measured in the top 5 cm from the mesocosms in the 2025 greenhouse study.

Response Variable/ Water Regime	Model Parameter	Coefficient (Standard Error)	Overall Model *P*-Value	Overall Model $R^{2\dagger}$	RSME†
CO_2					
IWD	Soil Eh*	1.00 (0.28)	<0.01	0.29	320.85
SFL	Soil Eh	1.07 (0.33)	<0.01	0.26	344.74
FL	Soil Eh	−0.03 (0.02)	0.22	0.05	26.89
CH_4					
IWD	Soil Eh	<0.01 (<0.01)	0.96	<0.01	0.02
SFL	Soil Eh	<0.01 (<0.01)	0.23	0.05	0.19
FL	Soil Eh*	<−0.01 (<0.01)	0.04	0.14	0.43
N_2O					
IWD	Soil Eh	<0.01 (<0.01)	0.44	0.02	0.10
SFL	Soil Eh*	<0.01 (<0.01)	0.03	0.15	0.07
FL	Soil Eh*	<0.01 (<0.01)	<0.01	0.24	0.05

*P < 0.05; †R^2, r-square; RSME, root square mean error.

Fluctuations of environmental conditions in the pedosphere impact soil-microbial mechanisms that lead to GHG production and multiple factors need to be considered to be able to efficiently capture and explain the variability of GHG fluxes [49].

3.7. Water Soluble Nutrients Change over Time

Understanding soil nutrient dynamics from different moisture regimes aids water management decisions and influences soil nutrients across numerous landscapes. Statistical analysis determined WS-Mg, -S, -Fe, -Mn, and -Zn differed by water regime over time, WS-K, -Ca, and -Na differed only over time and WS-P differed by water regime and differed over time ($P < 0.05$; **Table 5**). Throughout the study, WS-Ca, -K, and -Na were lowest on 12 and 25 February (DOY 43 and 56), spiked to the study-long maximum on 11 March (DOY 70), and WS-Ca and -K decreased during the final two weeks while WS-Na did not change (**Table 6**). The spikes observed on the third sampling date for WS-Ca, -K, and -Na occurred during the first dry cycle, but when the level of soil moisture was still above 0.30 $cm^3 \cdot cm^{-3}$ in the IWD and SFL mesocosms (**Figure 1**). The concentration of WS-Ca and -K in the FL mesocosms might have carried a large weighting factor in the observed maximum on 11 March sampling date (**Table 6**). Compost mineralization might have also influenced the increase of WS-Ca and -K observed on the third sampling date. The increase in VWC measured shortly after the third sampling date may have enhance adsorption of WS-Ca, -K, and -Na on the soil particles, which may otherwise be suspended in solution (**Figure 1**). The decrease in WS-Ca and -K on the final two sampling dates could be related to Ca and K bound to cation exchange sites on clay mineral edges during the dry cycle, and becoming exchangeable, limiting the fraction of nutrient considered as water soluble (**Figure 1**) [50]. The lower affinity of Na, compared to Ca and K, for negatively charged clay edges might have determined the lack of change of WS-Na reported during the last two sampling dates (**Table 6**).

Table 5. Analysis of variance summary of the effects of water-regime treatment, time (*i.e.*, sampling date), and their interaction on water-soluble nutrients [*i.e.*, phosphorus (P), potassium (K), calcium (Ca), magnesium (Mg), sodium (Na), sulfur (S), iron (Fe), manganese (Mn), zinc (Zn)] for the 2025 greenhouse study.

Soil Nutrient	Water Regime	Time	Water Regime × Time
P	<0.01	<0.01	0.09
K	0.27	<0.01	0.08
Ca	0.65	<0.01	0.11
Mg	0.28	<0.01	0.02
Na	0.18	<0.01	0.14
S	<0.01	<0.01	<0.01
Fe	<0.01	<0.01	<0.01
Mn	<0.01	<0.01	<0.01
Zn	0.91	0.22	0.66

In contrast to WS-Ca, -K, and -Na, WS-P differed by water regime and time (sample date, Table 5). Averaged among water regimes, WS-P was greatest on 11 and 25 March (DOY 70 and 84), and lowest at the end of the growing season, which was lower than initial WS-P and did not differ from the second measurement date (Table 6). Averaged among sampling dates, WS-P was greatest from the IWD treatment (4.1 $mg \cdot kg^{-1}$), and lowest from the SFL (3.5 $mg \cdot kg^{-1}$) and FL (3.2 $mg \cdot kg^{-1}$) moisture regimes, which was similar to what was hypothesized. Water soluble-P was likely greatest from the IWD moisture regime because the wetting and drying cycles created ideal conditions to release previously immobilized P bound to Ca, Mg, or Fe, which was supported by the increase in all three nutrients on the third measurement date (Figure 1; Table 6).

In contrast to WS-P, -Ca, -K, and -Na, WS-Mn, -Fe, -S, and -Mg differed by water regime over time ($P < 0.05$) with a similar general trend throughout the study period (Table 5; Figure 5). Water soluble-Mn, -Fe, -S, and -Mg among the FL, SFL, and IWD moisture regimes generally increased from 12 February to 11 March (DOY 43 to 70) and slightly decreased from 11 March to 2 April (DOY 70 to 92; Figure 5). Notably, Mn, Fe, and S were the only elements where differences within a sampling week were observed, and more differences were observed in order of most to least oxidizable elements (*i.e.* Mn > Fe > S) [50]. Thus, WS-Mn differed on more dates compared to WS-Fe or S because Mn is more susceptible to oxidation, which increased solubility during wet periods, with slighter changes in moisture or redox than Fe or S [47].

Table 6. Summary of the effect of time (*i.e.*, sample date) on water-soluble calcium (Ca), potassium (K), sodium (Na), and phosphorus (P) for the 2025 greenhouse study.

Sample Date	Day of Year	Soil Property ($mg \cdot kg^{-1}$)			
		Ca	K	Na	P
12 Feb	43	42 d[†]	37 c	26 c	3.3 b
25 Feb	56	48 d	37 c	34 b	3.2 bc
11 Mar	70	105 a	55 a	42 a	4.6 a
25 Mar	84	92 b	49 b	41 a	4.1 a
2 Apr	92	67 c	45 b	40 a	2.7 c

[†]Means within a soil property with different lower-case letters are different at $P < 0.05$.

Water soluble-Mn differed on 11 March, 25 March, and 2 April (DOY 70, 84, and 92), where the FL and SFL moisture regimes were similar to each other and greater than the IWD (Figure 5).

Variations in WS-Mn appear related to soil VWC, which can be observed on 11 March, 25 March, and 2 April (DOY 70, 84, and 92) where the IWD soil moisture is lower than SFL and FL, which could explain the lower WS-Mn from the IWD treatment (Figure 1; Figure 2; Figure 5). Water-soluble-Fe differed on two measurements, where the FL treatment was similar to the SFL, but lower than

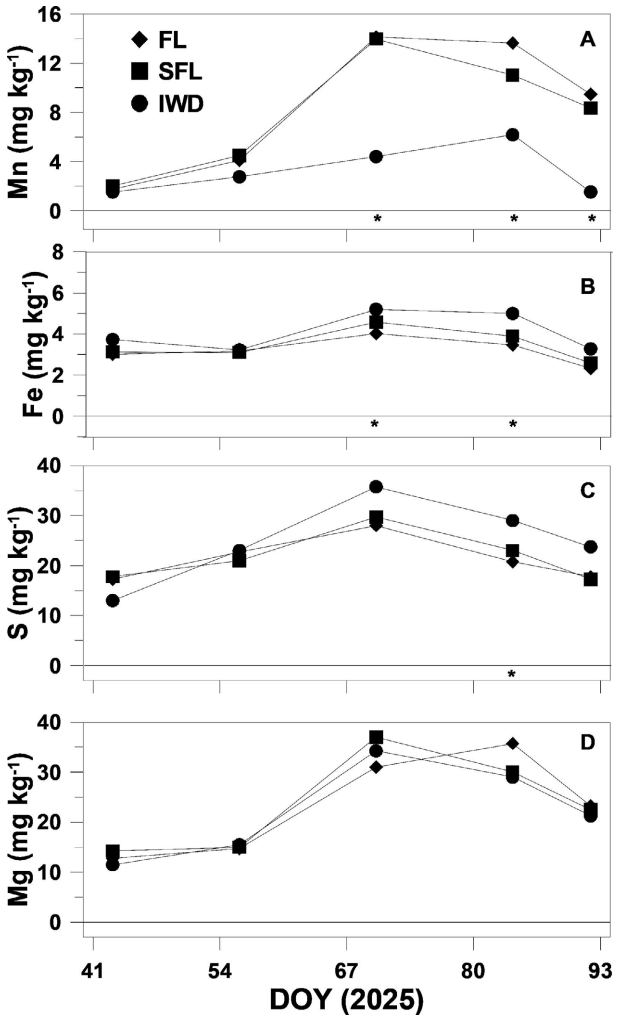

Figure 5. Water-soluble soil manganese (Mn, panel A), iron (Fe, panel B), sulfur (S, panel C), and magnesium (Mg, panel D) between day of year (DOY) among water regimes [*i.e.*, intermittent wetting and drying (IWD), flooded (FL), and seasonally flooded (S-FL)] for the 2025 greenhouse study. Lines connecting data points are for graphical representation only. Asterisks (*) below the zero line denote sample dates when a significant ($P < 0.05$) difference occurred among treatments.

the IWD on 11 and 25 March (DOY 70 and 84; Figure 5). The differences within a measurement date appear greatest to lowest based on the degree of soil moisture fluctuations prior to sampling. The larger fluctuation in soil moisture from the IWD regime could reduce Fe quicker than the FL and SFL regimes, which may explain the greater Fe from the IWD (Figure 1; Figure 5). Water-soluble-S differed only on 25 March (DOY 84) where the FL treatment was similar to the SFL, but lower than IWD, which was similar to the SFL water regime (Figure 5). While 25 March (DOY 84) was the sampling date with the lowest redox potential among the sampling dates, and while it was hypothesized the WS-S would be greatest from the FL treatment, the IWD cycles may mineralize more sulfur from increased organic matter decomposition than the flooded treatments (Figure 2) [50]. The increase of redox-active elements in the soil solution during the third sampling

date was temporally close to the N_2O peak reported from the SFL mesocosms, highlighting the potential correlation between environmental conditions, nutrient dynamics, and microbial processes (**Figure 3**, **Figure 5**). The significant differences between water regime over time for the redox-active elements highlight how water management practices can regulate biogeochemical cycles in the soil (**Table 5**, **Figure 5**).

In contrast to the hypothesis, WS-Mg fluctuated throughout the growing season, but did not differ within a measurement date (**Figure 5**). The variation of WS-Mg throughout the study was likely due to a combination of drying phases that concentrated WS-Mg, organic matter mineralization, or the exchange of magnesium from cation exchange sites with other nutrients with a larger affinity for exchange sites (*i.e.* Ca) [50]. Notably, WS-nutrient magnitudes and ranges throughout this study appear similar to a study conducted by [51] that evaluated biochar rate impacts on soil pH and WS nutrients on silt-loam soil in the greenhouse.

4. Conclusions

This study evaluated three different watering regimes (*i.e.*, IWD, SFL, and FL) on soil VWC, Eh, GHG fluxes and emissions, and WS nutrient concentrations over time in a greenhouse setting. Evaluated soil was considered low in SOM, and near toxic levels of Fe, but similar to soils cultivated for extensive periods of time. Recorded soil VWC and Eh were visually inversely related, as expected due to the relationship of water-logged soils decreasing soil Eh. Flooded mesocosms experienced the greatest VWC and lowest Eh, whereas IWD and SFL mesocosms followed similar patterns according to wetting and drying cycles.

Greenhouse gas fluxes were highly variable and related to water regime treatment. Carbon dioxide fluxes were significantly limited in the FL treatment, most likely due to the ponded water preventing atmospheric O_2 exchange. In the SFL and IWD treatments as the VWC decreased the CO_2 fluxes increased. Fluxes of N_2O showed a relationship to treatment and time, with fluxes increasing as the VWC alternated between wetting and drying, most likely due to nitrification-denitrification cycles. Methane fluxes only varied by treatment and not by time, and were greatest in the flooded treatments similar to the initial hypothesis. In accordance with that hypothesized, CO_2 emissions were significantly greater for IWD than SFL mesocosms, and greater for SFL than FL mesocosms, likely due to more aerobic conditions for IWD and SFL mesocosms allowing for CO_2 respiration. In contrast to that hypothesized, CH_4 and N_2O emissions did not differ between treatments, however, numerical differences were noted, potentially indicating the need for a longer study duration to evaluate CH_4 and N_2O emissions. Calculated GWP values differed between treatments, with the greatest GWP occurring in IWD mesocosms, and the least occurring in FL mesocosms, concluding VWC may impact GWP and carbon losses from soil when soils are dry. Linear regression analyses highlighted the relevance of soil Eh in regulating GHGs and the im-

portance of redox control mechanism as a potential tool to mitigate the impact of GHGs on the global climate. Water soluble soil properties, like Mn, Fe, S, and elements like P that are critical to plant growth were impacted by the implemented water regimes, which highlights the importance of understanding water management impacts on soil properties. The multidisciplinary approach used in the current study determined how water regime can impact many aspects of the biogeochemical cycle occurring in the soil, highlighting the necessity to expand current scientific knowledge and ground truth dataset to develop adequate mitigation practice to preserve the soil, water and air resources threatened by global warming.

Conflicts of Interest

The authors declare no conflicts of interest regarding the publication of this paper.

References

[1] Canadell, J.G., Monteiro, P.M.S., Costa, M.H., Cotrim da Cunha, L., Cox, P.M., *et al.* (2021) Global Carbon and Other Biogeochemical Cycles and Feedbacks. In: Masson-Delmotte, V., Zhai, P., Pirani, A., Connors, S.L., Péan, C., Berger, S., *et al*, Eds., *Climate Change* 2021: *The Physical Science Basis. Contribution of Working Group I to the Sixth Assessment Report of the Intergovernmental Panel on Climate Change*, Cambridge University Press, 673-816.

[2] Subke, J.A., Iglima, I. and Cotrufo, F. (2006) Trends and Methodological Impacts in Soil CO_2 Efflux Partitioning: A Meta-Analytical Review. *Global Change Biology*, **12**, 921-943.

[3] Rey, A. (2015) Mind the Gap: Non-Biological Processes Contributing to Soil CO_2 Efflux. *Global Change Biology*, **21**, 1752-1761. https://doi.org/10.1111/gcb.12821

[4] Wang, Z.P., DeLaune, R.D., Patrick Jr, W.H. and Masscheleyn, P.H. (1993) Soil Redox and Ph Effects on Methane Production in a Flooded Rice Soil. *Soil Science Society of America Journal*, **57**, 382-385. https://doi.org/10.2136/sssaj1993.03615995005700020016x

[5] Schlesinger, W.H. and Bernhardt, E.S. (2013) Wetland Ecosystems. In: Schlesinger, W.H. and Bernhardt, E.S., Eds., *Biogeochemistry*, Elsevier, 223-274. https://doi.org/10.1016/b978-0-12-385874-0.00007-8

[6] Hayatsu, M., Tago, K. and Saito, M. (2008) Various Players in the Nitrogen Cycle: Diversity and Functions of the Microorganisms Involved in Nitrification and Denitrification. *Soil Science and Plant Nutrition*, **54**, 33-45. https://doi.org/10.1111/j.1747-0765.2007.00195.x

[7] van Groenigen, J.W., Huygens, D., Boeckx, P., Kuyper, T.W., Lubbers, I.M., Rütting, T., *et al.* (2015) The Soil N Cycle: New Insights and Key Challenges. *Soil*, **1**, 235-256. https://doi.org/10.5194/soil-1-235-2015

[8] Dalal, R.C. and Allen, D.E. (2008) Greenhouse Gas Fluxes from Natural Ecosystems. *Australian Journal of Botany*, **56**, 369-407. https://doi.org/10.1071/bt07128

[9] Wild, M. and Liepert, B. (2010) The Earth Radiation Balance as Driver of the Global Hydrological Cycle. *Environmental Research Letters*, **5**, Article 025203. https://doi.org/10.1088/1748-9326/5/2/025203

[10] Trenberth, K.E. (2011) Changes in Precipitation with Climate Change. *Climate Re-*

search, **47**, 123-138. https://doi.org/10.3354/cr00953

[11] Dutta, H. and Dutta, A. (2016) The Microbial Aspect of Climate Change. *Energy, Ecology and Environment*, **1**, 209-232. https://doi.org/10.1007/s40974-016-0034-7

[12] Pittelkow, C.M., Adviento-Borbe, M.A., Hill, J.E., Six, J., van Kessel, C. and Linquist, B.A. (2013) Yield-Scaled Global Warming Potential of Annual Nitrous Oxide and Methane Emissions from Continuously Flooded Rice in Response to Nitrogen Input. *Agriculture, Ecosystems & Environment*, **177**, 10-20. https://doi.org/10.1016/j.agee.2013.05.011

[13] Arndt, J.L., Emanuel, R.E. and Richardson, J.L. (2016) Hydrology of Wetland and Related Soils. In: Vepraskas, M.J. and Craft, C.B., Eds., *Wetland Soils*, CRC Press, 39-104. https://doi.org/10.1201/b18996-5

[14] Li, H.J., Yan, J.X., Yue, X.F. and Wang, M.B. (2008) Significance of Soil Temperature and Moisture for Soil Respiration in a Chinese Mountain Area. *Agricultural and Forest Meteorology*, **148**, 490-503. https://doi.org/10.1016/j.agrformet.2007.10.009

[15] Kechavarzi, C., Dawson, Q. and Leeds-Harrison, P.B. (2010) Physical Properties of Low-Lying Agricultural Peat Soils in England. *Geoderma*, **154**, 196-202. https://doi.org/10.1016/j.geoderma.2009.08.018

[16] Wu, X., Wang, W., Xie, X., Yin, C., Hou, H., Yan, W., *et al.* (2018) Net Global Warming Potential and Greenhouse Gas Intensity as Affected by Different Water Management Strategies in Chinese Double Rice-Cropping Systems. *Scientific Reports*, **8**, Article No. 779. https://doi.org/10.1038/s41598-017-19110-2

[17] Yang, S., Liu, X., Liu, X. and Xu, J. (2017) Effect of Water Management on Soil Respiration and NEE of Paddy Fields in Southeast China. *Paddy and Water Environment*, **15**, 787-796. https://doi.org/10.1007/s10333-017-0591-1

[18] Banerjee, S., Helgason, B., Wang, L., Winsley, T., Ferrari, B.C. and Siciliano, S.D. (2016) Legacy Effects of Soil Moisture on Microbial Community Structure and N_2O Emissions. *Soil Biology and Biochemistry*, **95**, 40-50. https://doi.org/10.1016/j.soilbio.2015.12.004

[19] Lai, T.V. and Denton, M.D. (2017) N_2O and N_2 Emissions from Denitrification Respond Differently to Temperature and Nitrogen Supply. *Journal of Soils and Sediments*, **18**, 1548-1557. https://doi.org/10.1007/s11368-017-1863-5

[20] Vepraskas, M.J., Polizzotto, M. and Faulkner, S.P. (2016) Redox Chemistry of Hydric Soils. In: Vepraskas, M.J. and Craft, C.B., Eds., *Wetland Soils*, CRC Press, 105-132.

[21] Husson, O., Husson, B., Brunet, A., Babre, D., Alary, K., Sarthou, J.P., *et al.* (2016) Practical Improvements in Soil Redox Potential (Eh) Measurement for Characterisation of Soil Properties. Application for Comparison of Conventional and Conservation Agriculture Cropping Systems. *Analytica Chimica Acta*, **906**, 98-109. https://doi.org/10.1016/j.aca.2015.11.052

[22] Fiedler, S., Vepraskas, M.J. and Richardson, J.L. (2007) Soil Redox Potential: Importance, Field Measurements, and Observations. *Advances in Agronomy*, **94**, 1-54. https://doi.org/10.1016/s0065-2113(06)94001-2

[23] Altor, A.E. (2016) Biology of Wetland Soils. In: Vepraskas, M.J. and Craft, C.B., Eds., *Wetland Soils*, CRC Press, 133-163.

[24] Zhang, H., Hardy, D.H., Mylavarapu, R. and Wang, J.J. (2014) Mehlich-3. In: Sikora, F.J. and Moore, K.P., Eds., *Soil Test Methods from the Southeastern United States*, Southern Extension and Research Activity Information Exchange Group, 101-110. https://aesl.ces.uga.edu/sera6/PUB/MethodsManualFinalSERA6.pdf

[25] Della Lunga, D., Brye, K.R., Slayden, J.M., Henry, C.G. and Wood, L.S. (2021) Rela-

tionships among Soil Factors and Greenhouse Gas Emissions from Furrow-Irrigated Rice in the Mid-Southern, USA. *Geoderma Regional*, **24**, e00365. https://doi.org/10.1016/j.geodrs.2021.e00365

[26] Rogers, C.W., Brye, K.R., Smartt, A.D., Norman, R.J., Gbur, E.E. and Evans-White, M.A. (2014) Cultivar and Previous Crop Effects on Methane Emissions from Drill-Seeded, Delayed-Flood Rice Production on a Silt-Loam Soil. *Soil Science*, **179**, 28-36. https://doi.org/10.1097/ss.0000000000000039

[27] Rector, C., Brye, K.R., Humphreys, J., Norman, R.J., Gbur, E.E., Hardke, J.T., *et al.* (2018) N_2O Emissions and Global Warming Potential as Affected by Water Management and Rice Cultivar on an Alfisol in Arkansas, USA. *Geoderma Regional*, **14**, e00170. https://doi.org/10.1016/j.geodrs.2018.e00170

[28] Della Lunga, D., Brye, K.R., Slayden, J.M. and Henry, C.G. (2023) Evaluation of Site Position and Tillage Effects on Global Warming Potential from Furrow-Irrigated Rice in the Mid-Southern USA. *Geoderma Regional*, **32**, e00625. https://doi.org/10.1016/j.geodrs.2023.e00625

[29] Espinoza, L., Slaton, N. and Mozaffari, M. (2025) Understanding the Numbers on Your Soil Test Report. University of Arkansas Division of Agriculture. https://www.uaex.uada.edu/publications/pdf/FSA-2118.pdf

[30] Wang, J., Bogena, H.R., Vereecken, H. and Bruggemann, N. (2018) Characterizing Redox Potential Effects on Greenhouse Gas Emissions Induced by Water-Level Changes. *Vadose Zone Journal*, **17**, 1-13.

[31] Grundl, T., Haderlein, S., Nurmi, J. and Tratnyek, P. (2011) Introduction to Aquatic Redox Chemistry. *ACS Symposium Series*, **1071**, 1-14.

[32] Miele, F., Benettin, P., Wang, S., Retti, I., Asadollahi, M., Frutschi, M., Mohanty, B., Bernier-Latmani, R. and Rinaldo, A. (2023) Spatially Explicit Linkages between Redox Potential Cycles and Soil Moisture Fluctuations. *Water Resources Research*, **59**, e2022WR032328. https://doi.org/10.1029/2022wr032328

[33] Oo, A.Z., Win, K.T. and Bellingrath-Kimura, S.D. (2015) Within Field Spatial Variation in Methane Emissions from Lowland Rice in Myanmar. *SpringerPlus*, **4**, 145-155. https://doi.org/10.1186/s40064-015-0901-2

[34] Novara, A., Armstrong, A., Gristina, L., Semple, K.T. and Quinton, J.N. (2012) Effects of Soil Compaction, Rain Exposure and Their Interaction on Soil Carbon Dioxide Emission. *Earth Surface Processes and Landforms*, **37**, 994-999. https://doi.org/10.1002/esp.3224

[35] Slayden, J.M., Brye, K.R., Lunga, D.D., Henry, C.G., Wood, L.S. and Lessner, D.J. (2021) Site Position and Tillage Treatment Effects on Nitrous Oxide Emissions from Furrow-Irrigated Rice on a Silt-Loam Alfisol in the Mid-South, USA. *Geoderma Regional*, **28**, e00491. https://doi.org/10.1016/j.geodrs.2022.e00491

[36] Sey, B.K., Manceur, A.M., Whalen, J.K., Gregorich, E.G. and Rochette, P. (2008) Small-Scale Heterogeneity in Carbon Dioxide, Nitrous Oxide and Methane Production from Aggregates of a Cultivated Sandy-Loam Soil. *Soil Biology and Biochemistry*, **40**, 2468-2473. https://doi.org/10.1016/j.soilbio.2008.05.012

[37] Tokida, T., Miyazaki, T., Mizoguchi, M. and Seki, K. (2004) *In Situ* Accumulation of Methane Bubbles in a Natural Wetland Soil. *European Journal of Soil Science*, **56**, 389-396. https://doi.org/10.1111/j.1365-2389.2004.00674.x

[38] Luo, G.J., Kiese, R., Wolf, B. and Butterbach-Bahl, K. (2013) Effects of Soil Temperature and Moisture on Methane Uptake and Nitrous Oxide Emissions across Three Different Ecosystem Types. *Biogeosciences*, **10**, 3205-3219.

https://doi.org/10.5194/bg-10-3205-2013

[39] Gutenberg, L., Krauss, K.W., Qu, J.J., Ahn, C., Hogan, D., Zhu, Z., *et al.* (2019) Carbon Dioxide Emissions and Methane Flux from Forested Wetland Soils of the Great Dismal Swamp, USA. *Environmental Management*, **64**, 190-200. https://doi.org/10.1007/s00267-019-01177-4

[40] Hassett, E., Bohrer, G., Kinsman-Costello, L., Onyango, Y., Pope, T., Smith, C., *et al.* (2024) Changes in Inundation Drive Carbon Dioxide and Methane Fluxes in a Temperate Wetland. *Science of the Total Environment*, **915**, Article 170089. https://doi.org/10.1016/j.scitotenv.2024.170089

[41] Smith, K.A., Thomson, P.E., Clayton, H., Mctaggart, I.P. and Conen, F. (1998) Effects of Temperature, Water Content and Nitrogen Fertilisation on Emissions of Nitrous Oxide by Soils. *Atmospheric Environment*, **32**, 3301-3309. https://doi.org/10.1016/s1352-2310(97)00492-5

[42] Jin, Q., Liu, H., Xu, X., Zhao, L., Chen, L., Chen, L., *et al.* (2023) Emission Dynamics of Greenhouse Gases Regulated by Fluctuation of Water Level in River-Connected Wetland. *Journal of Environmental Management*, **329**, Article 117091. https://doi.org/10.1016/j.jenvman.2022.117091

[43] Canarini, A., Kiær, L.P. and Dijkstra, F.A. (2017) Soil Carbon Loss Regulated by Drought Intensity and Available Substrate: A Meta-Analysis. *Soil Biology and Biochemistry*, **112**, 90-99. https://doi.org/10.1016/j.soilbio.2017.04.020

[44] Lal, R. (2019) Carbon Cycling in Global Drylands. *Current Climate Change Reports*, **5**, 221-232. https://doi.org/10.1007/s40641-019-00132-z

[45] Nimon, K.F. and Oswald, F.L. (2013) Understanding the Results of Multiple Linear Regression: Beyond Standardized Regression Coefficients. *Organizational Research Methods*, **16**, 650-674.

[46] Wang, C., Lai, D.Y.F., Sardans, J., Wang, W., Zeng, C. and Peñuelas, J. (2017) Factors Related with CH_4 and N_2O Emissions from a Paddy Field: Clues for Management Implications. *PLOS ONE*, **12**, e0169254. https://doi.org/10.1371/journal.pone.0169254

[47] Malyan, S.K., Bhatia, A., Kumar, A., Gupta, D.K., Singh, R., Kumar, S.S., *et al.* (2016) Methane Production, Oxidation and Mitigation: A Mechanistic Understanding and Comprehensive Evaluation of Influencing Factors. *Science of the Total Environment*, **572**, 874-896. https://doi.org/10.1016/j.scitotenv.2016.07.182

[48] Smith, K.A., Ball, T., Conen, F., Dobbie, K.E., Massheder, J. and Rey, A. (2003) Exchange of Greenhouse Gases between Soil and Atmosphere: Interactions of Soil Physical Factors and Biological Processes. *European Journal of Soil Science*, **54**, 779-791. https://doi.org/10.1046/j.1351-0754.2003.0567.x

[49] Petter, F.A., Borges de Lima, L., Marimon, B.H.J., Alves de Morais, L. and Marimon, B.S. (2016) Impact of Biochar on Nitrous Oxide Emissions from Upland Rice. *Journal of Environmental Management*, **169**, 27-33. https://doi.org/10.1016/j.jenvman.2015.12.020

[50] Weil, R.R. and Brady, N.C. (2016) The Nature and Properties of Soils. 15th Edition, Pearson Education Inc.

[51] Brye, J.B., Gwaltney, L., Della Lunga, D. and Brye, K.R. (2024) Biochar Source and Rate Effects on Soil pH and Water-Soluble Nutrients over Time in Simulated Furrow-Irrigated Rice in the Greenhouse. *Journal of Rice Research and Developments*, **6**, 466-476. https://doi.org/10.36959/973/446